REVISION 3 OF R6, ITS BACKGROUND AND VALIDITY

R. A. Ainsworth[1], A. R. Dowling[2], I. Milne[3], A. T. Stewart[4]

The CEGB's defect assessment procedure, R6, first published in 1976 has been recently revised to take account of developments in fracture mechanics since that time. This paper discusses the background to the revisions, the validity of them and gives a brief introduction to the revised procedures.

INTRODUCTION

The CEGB defect assessment procedure, colloquially known as R6, was first published in 1976 (1) with revisions published in 1977, 1980 and 1986. The 1977 and 1980 revisions incorporated changes to include treatment for thermal and residual stresses and ductile tearing, and were based upon the failure assessment diagram devised for the 1976 issue. The 1986 revision, Rev. 3 (2), has major changes in all these aspects and this paper describes the background to these changes and their validition.

1 Berkeley Nuclear Laboratories, CEGB
2 Generation Development & Construction Division, CEGB
3 Central Electricity Research Laboratories, CEGB
4 South Western Region, CEGB

THE FAILURE ASSESSMENT DIAGRAM

The basis of the original R6 procedure was the failure assessment diagram, FAD. This took advantage of the observations of Dowling and Townley (3) that there were two limiting loading regimes to a flawed structure, one defined by linear elastic fracture conditions and one by plastic collapse. In the notation of R6 these were described respectively as

$$K_r = \frac{K_I}{K_{mat}} = 1 \qquad (1)$$

and

$$S_r = \frac{P}{P_c} = 1 \qquad (2)$$

where K_I is the applied stress intensity factor, K_{mat} is the appropriate value of fracture toughness, P is the applied load and P_c is the plastic collapse load. The FAD provided a means of interpolating between these two regimes via the generalised equation

$$K_r = f(S_r) \qquad (3)$$

In the original version of R6(1), $f(s_r)$ was based upon strip yielding models(4), and any allowance for strain hardening effects was incorporated empirically by defining S_r in terms of a flow stress, $\bar{\sigma}$, such that $P_c = P_c(a, \bar{\sigma})$ where a is the crack size.

In Revision 3 of R6(2) the concept of the FAD is retained, but $f(S_r)$ is replaced by $f(L_r)$ where

$$L_r = \frac{P}{P_y} \qquad (4)$$

and P_y is the yield limit load for the flawed structure, $P_y(a, \sigma_y)$, where σ_y is the yield stress. Strain hardening effects are incorporated explicitly by defining equations for $f(L_r)$ which are based upon estimates of the J integral. Three options of FAD are available, as follows.

Option 3

This is based directly upon the equivalence between the failure assessment diagram and a J integral analysis first identified by Chell(5). In this case the functional form, f_3 is

$$f_3(L_r) = \left\{\frac{J}{J_e}\right\}^{-\frac{1}{2}} \qquad (5)$$

where J and J_e are values of the J integral obtained for an elastic plastic and elastic analysis at the same load, L_r. Any method of calculating J may be used, but of course such methods are often elaborate, time consuming and expensive, and need to be validated. They are not satisfactory for general use, and for this reason options 2 and 1 were developed.

Option 2

One method of calculating J for use in equation 5 is to use the GE Scheme (6,7). There are several limitations to this (8) but the two most important ones are that there are only a limited number of (2-dimensional) geometries for which solutions are available and the solutions use the Ramberg Osgood law to characterise the materials stress strain curve. The first of these severely restricts the use of the scheme and the second can make the results inaccurate and user sensitive (8,9). To overcome these difficulties, Ainsworth (10) used a reference stress approach to reformulate the equations of Kumar et al (6) so that the actual stress strain curve of the material could be used rather than the Ramberg-Osgood representation. He also introduced pessimistic approximations to remove the geometry dependence. The form chosen for revision 3 of R6 was

$$f_2(L_r) = \left\{\frac{E\varepsilon_{ref}}{L_r\sigma_y} + \frac{L_r^3\sigma_y}{2E\varepsilon_{ref}}\right\}^{-\frac{1}{2}} \qquad (6)$$

where $\sigma_{ref}, \varepsilon_{ref}$ are co-ordinate points on the materials stress strain curve, $L_r = \sigma_{ref}/\sigma_y$ and E is Young's modulus. The first term describes the elastic and the fully plastic behaviour and the second term the transition through the small scale yielding regime (11).

Option 1

Some typical stress strain curves for a number of materials are plotted in Fig. 1, on normalised axes. The corresponding option 2 failure assessment curves of equation 6 are shown in Fig. 2. Also shown in Fig. 2 is the option 1 curve. This curve was constructed to have the same general shape as the option 2 curves, but to be biased towards their

lower bound. It was developed for situations where the stress strain data is not complete enough for use in equation 6 and it has the form

$$f_1(L_r) = \left(1 - 0.14 L_r^2\right)\left\{0.3 + 0.7 \exp\left(-0.65 L_r^6\right)\right\} \qquad (7)$$

It can be seen from Fig. 2 that equation 7 is particularly suitable for austenitic materials. It may also be used for ferritic materials but caution should be exercised where there is a lower yield plateau. In some extreme loading situations (e.g. pure tension) the lower yield plateau may be observed even in a cracked body (8). In these cases either equation 6 must be used or equation 7 should be limited to values of $L_r < 1.0$.

Plastic Collapse Limit

Equation 4, together with equations 5, 6 or 7 as appropriate, defines a continuous curve such that $K_r = 1$ where $L_r = 0$ and $K_r = 0$ at large L_r. This is consistent with J analysis but it provides no explicit facility to safeguard against overloading of uncracked ligaments or the operation of other plastic collapse mechanisms. To be consistent with earlier versions of R6 (1) and the observations of Dowling and Townley (3) the plastic collapse criterion is inserted as a cut-off on the FADs at a value $L_r = L_r^{max}$ given by

$$L_r^{max} = \frac{\bar{\sigma}}{\sigma_y} \qquad (8)$$

where $\bar{\sigma}$ is the flow stress appropriate to the material in question. Thus, equations 5, 6 and 7 apply only up to $L_r = L_r^{max}$ and thereafter $K_r = 0$. Typical values of L_r^{max} have been incorporated in Fig. 2 for the stress strain curves in Fig. 1, where $\bar{\sigma} = \frac{1}{2}(\sigma_y + \sigma_u)$ in each case, σ_u being the ultimate tensile stress.

Validation

The acceptance of the option 1 equation depends upon the validity of option 2. This has been validated extensively by comparison with option 3 FADs derived from J values obtained both experimentally and from finite element analysis of a number of test specimen geometries of different steels. The details of the validation are contained in reference 12, but can be summarised as follows.

Geometric effects were examined by testing 3 point bend, double edged notched tension, single edged notched tension (13) and centre cracked tension (12) specimens of austenitic steel, each with three different crack depths, 0.4, 0.6 and 0.8 of the width. The results, plotted in Figs. 3a and b, show no systematic geometric effect.

Specimen size effects were similarly examined, using 3-point bend specimens of A533B steel 10mm and 230mm thick (12). Both sizes of specimen were adequately represented by the Option 2 equation, Fig. 4.

The effects of the detail of the material's stress strain curve have been examined throughout a series of programmes, using compact tension and centre cracked panel geometries (12, 14, 15). The general conclusion was that the option 2 equation provided a sufficiently accurate solution for the steels studied, which included a strongly strain ageing carbon manganese steel tested over a temperature range from 20 to 300°C. In particular, for materials which exhibit a lower yield plateau, the option 2 equation provided a more accurate representation of a centre cracked panel specimen than an option 3 solution based upon finite element analysis where a stress strain representation was used which smoothed out the lower yield plateau (Fig. 5) (14).

Several comparisons have also been made between option 2 FADs and option 3 FADs derived from finite element solutions for a wide variety of geometries (10, 12, 14, 15, 16) and these show general consistency where the stress strain data is treated in the same way as for the finite element analyses.

TREATMENT OF THERMAL AND RESIDUAL STRESSES

In R6, stresses are characterised as σ^P or σ^S. The σ^P stresses are mechanically induced and arise in general as a response to the loading on the structure. They may also arise from thermal or residual welding strains where there is significant elastic follow-up. Thermal and residual stresses without significant elastic follow-up are classed as σ^S stresses. These stresses are self equilibrating in nature, and so play no role in plastic collapse failure (17). They have therefore to be treated differently from σ^P stresses.

Fig. 6 shows a plot of J/J_e against L_r for a structure loaded by σ^p stresses only, and by σ^p stresses superimposed on an existing σ^s stress. At low values of L_r the curve for the combined loading rises above that for the σ^p loading only, because at any given L_r the small scale plasticity effects due to the combined loading are greater than those due to the σ^p loading only. In order to bring the two curves in Fig. 6 into line a vertical shift is needed which depends upon the value of L_r.

The shift shown in Fig. 6 corresponds to a shift in the failure assessment curve through the equivalence of the FAD and J-estimates (5). In revision 2 of R6 this was allowed for by adjusting the calculated values of K_r only, keeping the value of S_r the same. Revision 3 of R6 adopts a similar technique. Analysis is performed using the chosen FAD, equation 5, 6 or 7, and the input is calculated as

$$L_r = L_r^p = \frac{\text{applied } \sigma^p \text{ load}}{\text{yield load}} \qquad (9)$$

$$K_r = K_r^s + K_r^p \qquad (10)$$

$$= \left\{ \frac{K_I}{K_{mat}} + \rho \right\} + \frac{K_I^p}{K_{mat}} \qquad (10a)$$

where the superscripts p and s denote quantities calculated for σ^p and σ^s stresses respectively.

The parameter ρ is to be thought of as part of K_r^s and must be calculated to provide the shift necessary to bring into line the two curves in Fig. 6. It depends upon the magnitude of both stress systems. Values of ρ suitable for general use have been calculated by Ainsworth (18) using reference stress techniques, and the concept of an equivalent mechanical load which produces the same deformation as the combined loading. These show a strong dependence on the value of the applied mechanical load. This dependence was approximated pessimistically for use in R6 Rev. 3 by using the maximum value for ρ at $L_r < 0.8$ and decreasing ρ to zero for $0.8 < L_r < 1.05$(12). The values given in R6 Rev. 3 are given as a function of the non-dimensional ratio $K_I^s/(K_I^p/L_r)$ as follows:

$$\rho = \rho_1 \qquad L_r < 0.8 \qquad (11a)$$

$$\rho = 4\rho_1(1.05 - L_r) \qquad 0.8 < L_r < 1.05 \qquad (11b)$$

$$\rho = 0 \qquad 1.05 < L_r \qquad (11c)$$

$$\rho_1 = 0.1x^{0.714} - 0.007x^2 + 0.0003x^5; \qquad x < 5.2 \qquad (11d)$$

$$\rho_1 = 0.25; \qquad x < 5.2 \qquad (11e)$$

$$x = K_1^s/(K_1^p/L_r) \qquad (11f)$$

Validation

This is mainly based upon comparisons of option 1 and option 2 FADs with option 3 FADs calculated using finite element methods, and adjusted to allow for the necessary value of ρ. The calculations all used a stress strain curve typical of an austenitic steel, and were performed using the BERSAFE finite element system (19) and its associated fracture mechanics methods for obtaining J (20). The comparisons are reported elsewhere (12, 18) and a typical result is shown in Fig. 7. Here, on the FAD, are plotted the results of Muscati (21) for a thick externally circumferentially cracked cyclinder subjected to an axial tension and a through-wall temperature gradient typical of a thermal shock loading. For mechanical loading only, and for modest amplitudes of thermal stress with mechanical loading superimposed, the finite element results lie close to but outside the R6 Rev. 3 FAD, as required. At larger thermal loads, the finite element results lie further outside. The implied extra pessimism for these situations results from treating the high peak thermal strains as elastically equivalent stresses. In practice plastic relaxation will take place. Although this can be treated by a more sophisticated form of analysis (22) such a treatment is beyond the scope of simplified procedures. Note that to calculate L_r, the limit load for the pipe geometry was taken as $(2/\sqrt{3})\,\sigma_y$ times net section area. This may not be sufficiently accurate, especially for short cracks and this may explain why some points lie just inside the FAD for mechanical loading only.

Some validation has also been obtained by performing a post test analysis on a pressure vessel test which had a crack situated in the residual stress field created by a non-stress relieved repair weld

(12, 23). The details of this will be summarised later.

ANALYSIS CATEGORIES AND TREATMENT FOR DUCTILE TEARING

The treatment for ductile tearing is conditioned by the available material toughness data and the desire or need to make allowances for tearing. In R6 Rev. 3 three categories of analysis may be performed, depending upon the relevant definition of K_{mat}. Suitable definitions are contained in R6 Rev.3, based upon state of the art understanding of fracture (24) and the CEGB J test procedure (25). These are listed in Table 1. The analysis category is therefore governed by the choice of K_{mat} in the calculation of K_r for the structure (equation 10). The maximum loading conditions permitted by each category of analysis is termed the limiting condition.

Category 1

This is a single point analysis, at the initial crack length, a_o, and load of interest, designed to avoid crack initiation. Thus, for brittle fracture mechanisms K_{mat} is defined by K_{1C} or K_C (Table 1), in which case K_r is given by K_I/K_{1C} or K_I/K_C as appropriate. For ductile cracking mechanisms,whose initiation is characterised by $K_{0.2}$ (Table 1), $K_r = K_I/K_{0.2}$. Failure is avoided if when plotted on the FAD the point of interest (L_r, K_r) lies inside the failure assessment line, and the limiting condition occurs when this point lies on the assessment line.

Category 3

This is a detailed ductile tearing analysis designed to evaluate against a potential ductile instability condition. Analysis is carried out as a function of crack extension, Δa, at the load of interest with both L_r and K_r being updated as necessary. The value of K_{mat} is obtained from the J resistance curve $K_{mat} = K_{\mathcal{R}}(\Delta a) = \{E^1 J(\Delta a)\}^{\frac{1}{2}}$ (Table 1) and co-ordinate points $L_r K_r$ are plotted on the FAD as a function of postulated crack extension (Fig. 8). If at the applied load a part of this locus falls within the failure assessment line the structure can be said to be stable. The limiting condition is when the locus just touches the failure assessment line. This may be at an angle to the assessment line as at A in Fig. 8,

where the available J (Δa) data is over a restricted range of crack extension, or at a tangency condition. This latter condition defines the load for load controlled instability (B in Fig. 9).

Category 2

The limiting conditions for categories 1 and 3 analyses make no allowance for any factors or margins deemed necessary for safe operation. The user is required to determine these separately after performing a sensitivity analysis to study the effects of variations in the input data, taking into account such things as the potential failure mechanism and the validity of the data. The main objectives are to ensure that the margin selected is sufficient to safeguard against extreme sensitivity in some parameters (possible cliff edge effects) and to establish whether or not the results are sensitive to the input. In a situation of ductile tearing, such lack of sensitivity is obtained where there is a large difference between the crack driving forces and the materials resistance to cracking. This occurs when there is a large difference in slope between the locus derived following a category 3 analysis and the failure assessment line at the point of interest and this feature is utilised in a category 2 analysis.

The category 2 analysis is a simplified tearing analysis performed at two points only, one at $K_{0.2}$ and one at K_g, the maximum toughness available from valid specimen data at Δa_g (Table 1). Load factors F^L_O and F^L_g are calculated for the respective assessment points, the generalised load factor F^L being defined for any assessment point as

$$F^L = \frac{\left\{\begin{array}{l}\text{load to place assessment point on failure}\\ \text{assessment line}\end{array}\right\}}{\text{Load of interest}} \qquad (12)$$

The limiting condition for a category 2 analysis is defined for 2 sets of conditions:

$$F^L_g > 1.1 \quad ; \quad F^L_g/F^L_O = 1.2 \qquad (13a)$$

$$F^L_g = 1.1 \quad ; \quad F^L_g/F^L_O > 1.2 \qquad (13b)$$

Thus if $F^L_g > 1.1$ and $F^L_g/F^L_O > 1.2$ the criteria are satisfied.

The category 2 criteria were chosen to ensure that

there is a 10% margin on load to extend the crack by Δa_g and that the difference between the applied crack during force and the materials resistance to cracking is sufficient to make the result relatively insensitive to variations in the resistance curve data. This relative sensitivity is shown schematically in Fig. 9, as a plot of tan α versus F^L_g/F^L_o. The angle α is an inverse measure of the angle between the category 3 locus and the failure assessment line at Δa_g (12) and it can be seen that tan α becomes insensitive to the ratio of F^L_g/F^L_o at values of this ratio greater than 1.2.

At the limit of F^L_g=1.1 the necessary condition for F^L_g/F^L_o requires that F^L_o<1.0 and implies that cracking has initiated. The amount of cracking in this limiting condition is, however, small and of no structural significance. The margin against instability is ensured by the imposed value of F^L_g/F^L_o which requires K_r at Δa_g to be much lower than K_r at a_o. This normally requires a steep resistance curve. Under these conditions there is no benefit to be gained from investigating further the sensitivity of the results to changes in the input data except to demonstrate that such changes do not cause a violation of the required limiting conditions. The sensitivity analysis required of a category 2 analysis is therefore simpler than required elsewhere. Failure to meet the category 2 requirements does not mean that other requirements cannot be met. They may be met either by performing a more elaborative sensitivity analyses, or by imposing restrictions on operating conditions, or by refining other parts of the analysis.

Limitations

Analysis Categories 2 and 3 allow advantage to be taken of the increase in toughness which occurs in many materials as tearing proceeds. However, ductile tearing may interact with other forms of cracking, such as fatigue, or it may precede brittle fracture. Caution must be exercised in such cases. For example, in fatigue, the fatigue crack growth rate may increase as fatigue interacts with tearing. Under these circumstances, it may be advisable for the user to limit himself to a Category 1 analysis. For the situation of ductile-brittle transition there is a potential cliff edge effect. In this situation, although the enhanced toughness value up to the onset of the brittle fracture (K_C or K_g,

Table 1) may be used in the analysis, the user may feel advised to impose larger factors against the limiting condition than he would in the absence of the ductile brittle transition. Advice on the treatment of these and other factors which may influence the result is contained in the R6 Rev. 3 document.

ASSESSMENT PROCEDURES

The 14 main sections and a number of supporting Appendices currently available in R6 Rev. 3 are listed in Table 2. The sections detail the major steps which must be followed when using the procedures, whereas the appendices are advisory, giving guidance on the different aspects of the analysis. The first few sections are introductory and the last, the fourteenth, outlines the status of various elements of the analysis: these have already been discussed. The main analysis steps as set out in Section 4 of R6 are easily followed by means of a flow chart (2). The steps listed below are a simplification of those in R6 Rev. 3.

1. Define and categorise all loads and stresses on the defective component. A distinction is made between loads which contribute to plastic collapse and loads which do not and these are categorised as σ^P and σ^S stresses, respectively.

2. Determine the material tensile properties σ_y, σ_u and $\bar{\sigma}$, and if needed the full stress-strain curve.

3. Select and define the FAD. This involves calculating L_r^{max} (eqn. 8) and defining the assessment curve (eqns. 5,6,7), the selection of which depends on the available stress-strain data (for eqn. 5 and 6) and the availability of a J-solution (for eqn. 6).

4. Characterise the shape and size of the flaw. The flaw shape must be characterised as one for which stress intensity factor and limit load solutions are available or can be calculated. For category 2 and 3 analyses it is necessary to characterise not only the initial flaw size but also that after some ductile growth, taking due account of the proximity of other flaws and surfaces.

5. Select the category of analysis. The three categories have been outlined earlier and the selection is influenced by the type and extent of toughness data available.

6. Define fracture toughness, either initiation toughness only (for category 1) or resistance curve data (for category 2,3).

7. Calculate L_r at the applied loads and crack size(s) of interest

$$L_r = \frac{\text{total applied load giving rise to } \sigma^P \text{ stresses}}{\text{plastic yield load of the flawed structure}}$$

8. Calculate K_r as above. In its general form

$$K_r = K_r^P + K_r^S$$

$$K_r^P = K_1^P/K_{mat};\ K_r^S = K_1^S/K_{mat} + \rho$$

9. Plot all points on the FAD.

10. Assess the significance of the results. For a category 1 analysis a single assessment point is calculated and failure is avoided if this is inside the failure assessment curve. For a category 2 analysis, the positions of the two assessment points relative to the curve must be such as to satisfy inequalities (12a and 12b). For a category 3 analysis the locus of assessment points as a function of crack extension should fall inside the curve over some part of its length. For all categories the significance of the result should be assessed by performing a sensitivity analysis on the load factors as functions of the input assumptions, calculations and materials data. Failure to obtain a satisfactory margin using one category of analyses does not imply that all categories will be unsatisfactory. Margins may also be improved by refining the analysis in other aspects, and even by modifying the operating conditions for the structure.

The above step-by-step procedure is simple to follow and allows the R6 approach to be applied in a consistant way in practice. However, the individual steps sometimes require sophisticated data collection or analysis and to provide guidance for this R6 contains 8 Appendices (see Table 2). The contents of these are briefly summarised below.

1. Information and methods for determining fracture toughness data.

2. Advice and sample solutions for limit analysis.

3. Methods for determining stress intensity factors.

4. Evaluation of interactions between σ^P and σ^S stresses.

5. Description of computer programs available within the CEGB for performing R6 assessments or parts thereof.

6. Procedures for including fatigue and environmentally assisted crack growth in an assessment.

7. Treatment of loadings giving rise to other than simple opening (mode I) conditions at the crack tip.

8. A specific FAD for carbon-manganese (mild) steels developed using the principles of option 2 but for use when detailed stress-strain data are unavailable.

GENERAL VALIDATION

Validation of the equations used to define the FADs both in the presence and absence of σ^S stresses has already been discussed. This section will summarise the details of a validation exercise performed on four structures which were tested to failure (12). The objective is to show that the procedures as followed in section 4 of R6 Rev. 3 provide adequate margins against the limiting conditions specified for the different categories of analysis. For this to be achieved unambiguously, only well defined test results and suitable input data may be considered.

The four tests analysed are

1. A CEGB pressure vessel test containing a semi-elliptical axial external crack in the cylindrical shell. This test was used in a predictive round robin exercise under the auspices of EGF (26).

2. A second pressure vessel test in the same programme, with a similar crack in a stress relieved submerged arc seam weld experiencing the residual

stress field of an adjacent non-stress relieved repair weld. This was also used in the EGF predictive round robin exercise (23).

3. The pressure vessel test at ORNL, designated HSST V8A, with an external crack in a weld metal specially degraded to have a low upper shelf Charpy energy level (27).

4. A bend test on an austenitic pipe containing a circumferential crack, performed at Battelle (28).

These tests have been subjected to exhaustive predictive analysis, using a variety of techniques (8) (27) and best estimate data. This is not the requirement here, however. In this case the data should be used in its intended form for R6 Rev. 3, to produce realistically based pessimistic values for the quantities L_r and K_r. If the analysis is then performed at the measured failure load, the assessment points should all fall outside the failure assessment line. These would correspond to load factors < 1, the inverse of which would give the factor of reserve obtained for that specific test.

The basis of all analyses was a category 3 analysis and the details are contained elsewhere (12). For tests 1, 3 and 4 the analysis was straightforward. For test 2, however, the residual stress profile was such that very high values of K_r^s were obtained at the region on the crack front located in the surface of the vessel. This necessitated analysing for two locations on the crack front, the deep point and the surface intersecting point. In this test failure was by leakage, the crack having grown through the ligament. This meant that a successful analysis required only that the category 3 locus for the deep point fell outside the failure assessment line. In the event, both loci fell outside the line, that for the deep point being the more remote indicating that the failure conditions were correctly ranked.

Figs. 10a,b,c and d show how the results were plotted on the relevant FADs and that all tests were successful. The factors of reserve obtained from these Figs. are listed in Table 3, along with other relevant information.

CONCLUDING COMMENTS

The main objectives in developing R6 were to produce a procedure which had the following attributes:

1. Relative simplicity with standardised rules allowing for consistency of application.

2. Ease of manipulation so that a large number of variables like crack location, material properties, flaw characterisation, loading regimes, etc. could be analysed quickly and cheaply, and so facilitate objective judgement of the necessary margins by use of a sensitivity analysis.

3. The capability of analysing for special circumstances, incorporating empirical solutions where necessary and allowing for development as and when new information became available.

4. Good validation so that together with the consistency of application authoritative bodies could accept the results without requiring further validation.

Revision 3 of R6 is now the most modern version, and incorporates the most important developments in fracture mechanics which were current up to April 1985. Further development is in hand, as a continuing programme, particularly in respect of computerisation, the treatment of thermal and residual stresses, leak before break analysis, the treatment of scattered material toughness data and in validation. The main changes incorporated in Revision 3 centre around the facility to treat the materials stress strain data explicitly. It is felt that this particular aspect is an important advance in fracture mechanics methodology.

ACKNOWLEDGEMENTS

The work was done within the Technology Planning and Research Function and Generation Development and Construction Division of the Central Electricity Generating Board and is published by permission of the CEGB.

REFERENCES

1. Harrison, R. P., Loosemore, K. and Milne, I, Assessment of the Integrity of Structures Containing defects, CEGB report R/H/R6, 1976.

2. Milne, I., Ainsworth, R. A., Dowling, A. R. and Stewart, A. T., Assessment of the integrity of structures containing defects, CEGB Report R/H/R6 Rev. 3, 1986.

3. Dowling, A. R. and Townley, C. H. A., Int. J. of Press. Vess. & Piping, vol. 3 1975 p.77.

4. Bilby, B. A., Cottrell, A. H. and Swinden, K. H., proc. Roy. Soc. vol. A272 1963 p. 304.

5. Chell, G. G., ASTM STP 668, p. 581-605 1979.

6. Kumar, V., German, M. D. and Shih, C. F., An Engineering approach to Elastic Plastic Fracture Analysis, EPRI report NP-1931 1981.

7. Bloom, J. M., ASTM STP 803 1983 p. II206-II238.

8. Milne, I., The state of the art in assessing structural integrity, proc. of Int. Conf. on Fracture control of engineering structures, ECF6, paper nr 150, 1986.

9. Milne, I., Int. J of Press. Vess. & Piping Vol. 13, 1983 p. 107.

10. Ainsworth, R. A., Eng. Fract. Mech. vol. 19 1984, p. 633-642.

11. Ainsworth, R. A., Milne, I., Dowling, A. R. and Stewart, A. T., Assessing the integrity of structures containing defects by the failure assessment diagram approach of the CEGB, proc. of ASME PVP and Computer Engineering Division Conference, Chicago 1986.

12. Milne, I., Ainsworth, R. A., Dowling, A. R., Stewart, A. T., Assessment of the integrity of structures containing defects, Validation CEGB report 1986.

13. Akhurst, K. N. and Milne, I., Int. Conf. on Application of fracture mechanics to materials and structures, Freiburg 1983.

14. Gates, R. S., Gladwin, D. N., Bradford, R. and Green, G., Effects of geometry on failure assessment diagrams for C-Mn steels: a comparison of CCP and CT geometries, CEGB report SWR/SSD/0622/N85 1986.

15. Green, G., Gladwin, D. N., Bradford, R. and Stewart, A. T., Strain hardening failure assessment diagrams derived from C-Mn steel compact tension specimens; implications of experimental and analytical results. CEGB report SWR/SSD/0491/N/84 1984.

16. Ainsworth, R. A., Chell, G. G. and Milne, I. proc. of CSNI/NRC, Workshop on ductile piping fracture mechanics, San Antonio Texas 1984.

17. Chell, G. G. and Ewing, D. J. F., Int. J. of Fracture vol. 13 1977 p. 467.

18. Ainsworth, R. A., The treatment of thermal and residual stresses in fracture assessments to be published in Eng. Fract. Mech.

19. BERSAFE, Users guides, CEGB Berkeley 1983.

20. Hellen, T. K., The use of finite element techniques in post yield fracture mechanics, CEGB report TPRD/B/0573/R85 1985.

21. Muscati, A., Elastic plastic fracture analyses of a thick cylinder subjected to combined thermal and mechanical loading, CEGB report SWR/SSD/0626/N85, 1985.

22. Chell, G. G., A J estimation procedure for combined mechanical, thermal and residual stresses. CEGB report TPRD/L/2930/N85 1985.

23. Knee, N., Experimental results and analytical predictions for failure in a weld repaired test pressure vessel (EGF phase IV) to be published.

24. Milne, I. and Curry, D. A., ASTM STP 803 1983, p. II 278-II290.

25. Neale, B. K., Curry, D. A., Green, G., Haigh, J. R. and Akhurst, K. N., A procedure for the determination of the fracture resistance of ductile steels, Int. J. of Press. Vess. & Piping Vol. 20 1985 p. 155-179.

26. Milne, I. and Knee, N., Report on EGF task group exercise in predicting ductile instability, phase II, experimental cracked pressure vessel. CEGB report TPRD/L/2771/N84 1985.

27. Bryan, R. H., Bass, B. R., Bryson, J. W. and Merkle, J. G. in Light Water Reactor Structural Integrity, ed. by K. E. Stahlkopf and L. E. Steele, 1984 p. 175-210.

28. Wilkowski, G. M., Ahmad, J., Barnes, C. R., Brook, D., Kramer, G., Landow, M., Marshall, C. W., Maxey, W., Nakagaki, M., Scott, P., Papaspyropoulos,V., Pasupathi, V. and Popelar, C., Degraded piping program - Phase II vol. 2 NUREG/CR-4082 1982.

SYMBOLS

$a, (a_o)$	crack size, (initial)
$\Delta a, (\Delta a_g)$	ductile crack extension (valid limit, Table 1)
E	Young's modulus
ε_{ref}	reference strain, uniaxial strain at stress, σ_{ref}
$F^L, (F^L_o, F^L_g)$	Factor on load (at a_o, at $a_o + \Delta a_g$)
FAD	Failure assessment diagram
$J, (J_e)$	J integral (elastically calculated)
$J\ (\Delta a)$	J resistance curve (Table 1)
$K_1, (K^p_1, K^s_1)$	Applied stress intensity factor (for σ^p stresses, for σ^s stresses)
K_{mat}	material's toughness parameter (see Table 1)
$K_r, (K^p_r, K^s_r)$	ratio K_1/K_{mat} (for σ^p stresses, for σ^s stresses including ρ)
$L_r (L_r^{max})$	load/yield load (max permitted)

$P, (P_y, P_c)$	load (yield limit load, collapse limit load)
ρ_1	plasticity interaction term for $\sigma^p + \sigma^s$ loading
S_r	load/collapse load (1)
σ^p	stresses produced from mechanical loads
σ^s	stresses produced from thermal or residual strains
σ_{ref}	reference stress = $L_r \sigma_y$
$\sigma_y, (\bar{\sigma}, \sigma_u)$	yield or proof (flow, ultimate) tensile stress

TABLE 1 MATERIAL TOUGHNESS DEFINITIONS

K_{Ic}	Linear elastic plane strain fracture toughness meeting requirements of national standards
K_c	toughness at onset of brittle fracture, where non-valid. May be derived from J analysis
$K_{0.2}$	toughness corresponding to 0.2mm of tearing and/or blunting in a ductile fracture test
K_g	toughness at Δa_g of tearing where Δa_g is limit permitted by validity rules (25), where brittle fracture follows tearing Δa_g corresponds to the minimum crack extension obtained
$K_{\Omega(\Delta a)}$	toughness as a function of ductile tearing,

$K_{0.2}, K_g, K_{\Omega(\Delta a)}$ must be derived from J(Δ a) resistance curve data (25).

TABLE 3 VALIDATION TEST RESULTS

Test	Loading	Measured quantities	Reserve factor on R6 Rev.3 analysis
CEGB p.v. test A533B	pressure only	Max. pressure	1.11
CEGB p.v. test SA weld repair	pressure + residual stress	initiation pressure	1.34 (1.23 surface)
		Max. pressure	1.34 (1.27 surface)
ORNL p.v. test SA weld	pressure only	Max. pressure	1.16
Battelle test on austenitic pipe	bending moment	initiation load	1.18
		Max. load	1.22

TABLE 2 CONTENTS OF R 6 REV. 3

Sections

Appendices

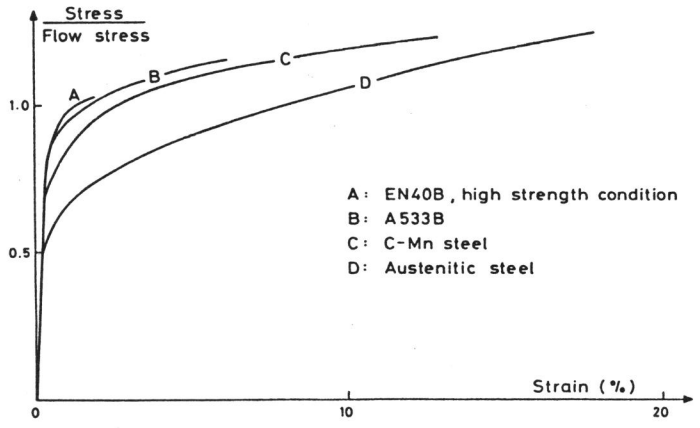

Fig. 1 Typical stress-strain curves

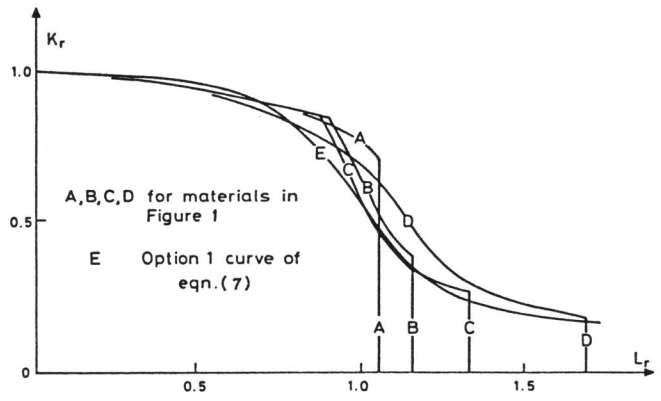

Fig. 2 Option 2 FADs

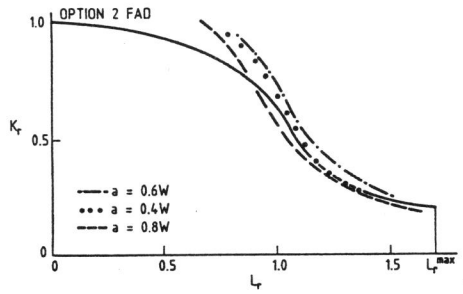

Fig. 3a Option 2 validation, austenitic steel, DENT geometry

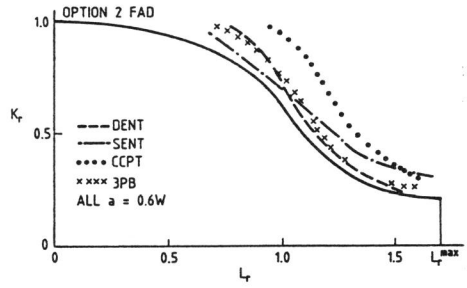

Fig. 3b Option 2 validation, austenitic steel

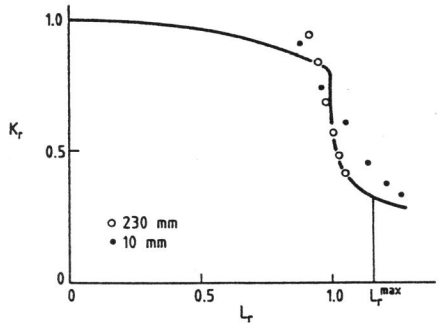

Fig. 4 Option 2 validation, specimen size

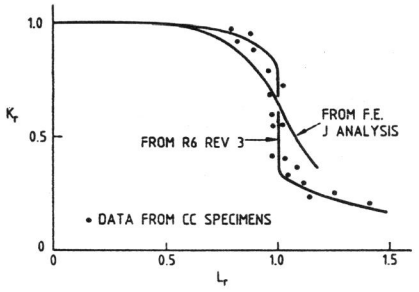

Fig. 5 FADs for C-Mn steel and tensile test results

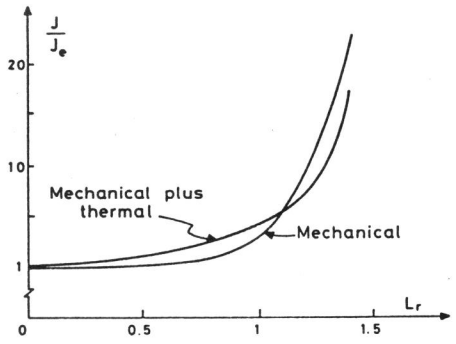

Fig. 6 Effect of σ^S stresses on J

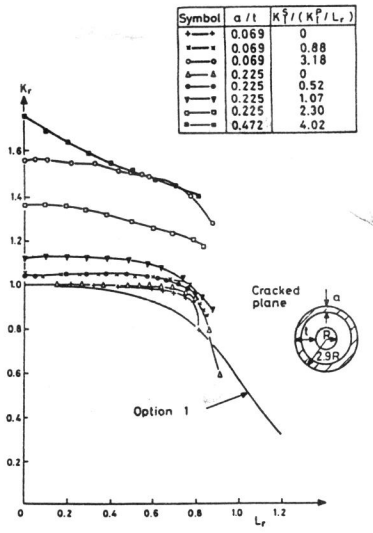

Fig. 7 Validation of σ^S treatment

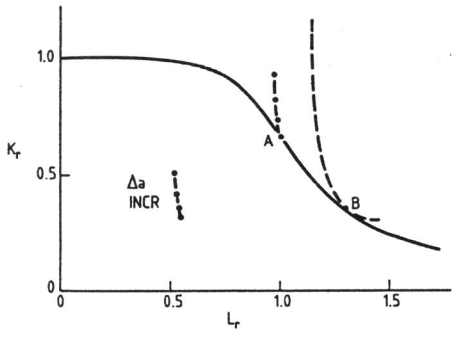

Fig. 8 Category 3 analysis

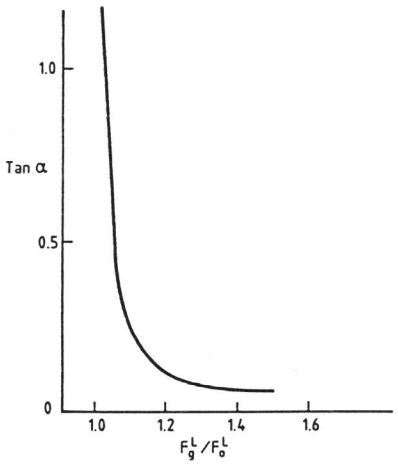

Fig. 9 Basis of cat. 2 criteria

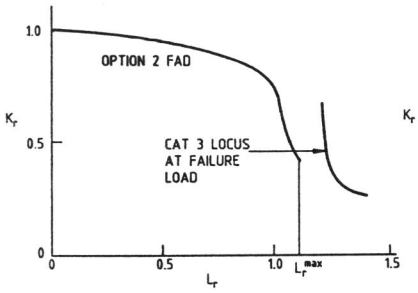

Fig. 10a Validation, test 1

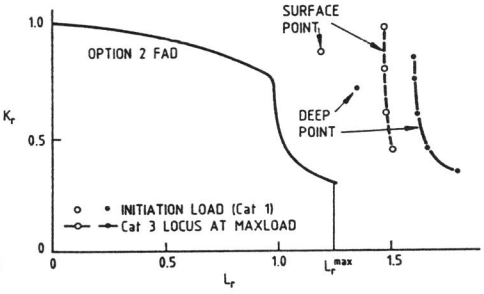

Fig. 10b Validation, test 2

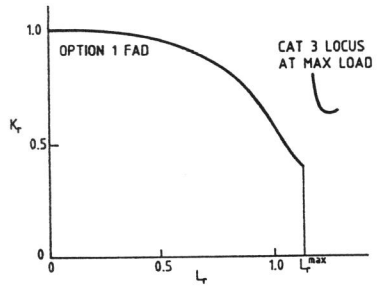

Fig. 10c Validation, test 3

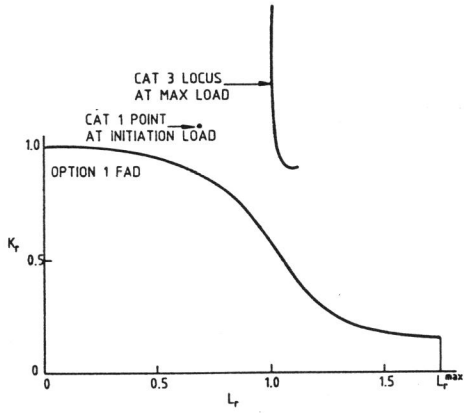

Fig. 10d Validation, test 4